Available online at www.sciencedirect.com
ScienceDirect
Journal of Computational Physics 218 (2006) 1–18
JOURNAL OF COMPUTATIONAL PHYSICS
www.elsevier.com/locate/jcp

Partial moment entropy approximation to radiative heat transfer

Martin Frank [a,*], Bruno Dubroca [b], Axel Klar [a]

[a] *Fachbereich Mathematik, TU Kaiserslautern, Erwin-Schrödinger-Str., 67663 Kaiserslautern, Germany*
[b] *MAB, Université Bordeaux I, Cours de la Libération, 33405 Talence, France*

Received 15 September 2005; received in revised form 6 January 2006; accepted 24 January 2006
Available online 7 March 2006

Abstract

We extend the half moment entropy closure for the radiative heat transfer equations presented in Dubroca and Klar [B. Dubroca, A. Klar, Half moment closure for radiative transfer equations, J. Comput. Phys. 180 (2002) 584–596] and Turpault et al. [R. Turpault, M. Frank, B. Dubroca, A. Klar, Multigroup half space moment approximations to the radiative heat transfer equations, J. Comput. Phys. 198 (2004) 363–371] to multi-D. To that end, we consider a partial moment system with general partitions of the unit sphere closed by an entropy minimization principle. We give physical and mathematical reasons for this choice of model and study its properties. Several numerical examples in different physical regimes are presented.

Keywords: Radiative transfer equations; Moment methods; Entropy minimization; Half fluxes

1. Introduction

In recent years the interest in numerically tractable approximations to the radiative heat transfer equations has drastically increased. Applications range from industrial cooling processes (e.g. glass cooling) over astrophysics to combustion (e.g. in gas turbine combustion chambers). Since radiative heat transfer (RHT) often plays a role in complex physical situations involving for example fluid flow and chemical reactions, one is interested in substituting the system of integro-differential equations describing RHT by a mathematically less complicated, yet accurate, approximate model. Examples of such approximate models are diffusion approximations [18], higher order diffusion approximations like P_N and SP_N equations (cf. [20,19] and references therein), and moment models [38,1,21].

The model that we present in this paper is a further development of the one-dimensional model introduced in [9] and developed in [41,43]. By using half moments, i.e., by averaging the radiative intensity over the directions going to the left and to the right separately, one can capture highly anisotropic physical situations. In one-dimensional numerical experiments the half moment model has shown to be very accurate at a low computational cost [9,8]. It is our purpose in this paper to extend this model to several space dimensions.

* Corresponding author. Tel.: +49 6312054486; fax: +49 6312054986.
E-mail addresses: frank@mathematik.uni-kl.de (M. Frank), Bruno.Dubroca@math.u-bordeaux.fr (B. Dubroca), klar@mathematik.uni-kl.de (A. Klar).

0021-9991/$ - see front matter
doi:10.1016/j.jcp.2006.01.038

We consider the RHT equations in a domain D in $\mathbb{R}^3$:

$$\rho_m c_m \partial_t T - \nabla \cdot (k \nabla T) = \int_{\mathscr{S}} \int_0^\infty \kappa (I_\nu - B_\nu(T)) \, \mathrm{d}\nu \, \mathrm{d}\mathbf{\Omega}, \tag{1.1}$$

$$\forall \mathbf{\Omega} \in \mathscr{S}, \ \forall \nu > 0 : \frac{1}{c} \partial_t I_\nu + \mathbf{\Omega} \cdot \nabla I_\nu = \sigma \left(\frac{1}{4\pi} \int_{\mathscr{S}} I_\nu \, \mathrm{d}\mathbf{\Omega} - I_\nu \right) + \kappa (B_\nu(T) - I_\nu). \tag{1.2}$$

In these equations, $I_\nu(\boldsymbol{x}, t, \mathbf{\Omega})$ denotes the radiative intensity at point $\boldsymbol{x} \in D$, time t, frequency ν, traveling into direction $\mathbf{\Omega} \in \mathscr{S}$, where $\mathscr{S}$ is the unit sphere in three dimensions. Furthermore, $T(\boldsymbol{x},t)$ is the material temperature. The heat conductivity is denoted by k. Although the absorption coefficient κ and the scattering coefficient σ generally depend on the frequency, we want to assume in the following that they are constant. How to handle frequency-dependent coefficients was shown in a previous paper [43]. Frequency-dependent quantities are marked with a subscript ν. Here, B_ν is the Planck equilibrium distribution,

$$B_\nu(T) = \frac{2h\nu^3}{c^2} \frac{1}{\exp(\frac{h\nu}{kT}) - 1}. \tag{1.3}$$

By $\langle B(T) \rangle$ we denote the Planckian integrated over all frequencies and directions,

$$\langle B(T) \rangle = \int_{\mathscr{S}} \int_0^\infty B_\nu(T) \, \mathrm{d}\nu \, \mathrm{d}\mathbf{\Omega} = aT^4, \tag{1.4}$$

where we have used Stefan's law. The parameter $a = \frac{2\pi^5 k^4}{15h^3c^2}$ is Stefan's constant.

We supplement this system with the following boundary conditions. For the material temperature we consider the heat flux through the boundary due to advection,

$$k\boldsymbol{n} \cdot \nabla T = h_B(T_b - T). \tag{1.5}$$

Here, T_b is the outside temperature and α is the hemispheric emmisivity/absorptivity. Furthermore, we prescribe semi-transparent boundary conditions for the ingoing radiation,

$$I_\nu(\mathbf{\Omega}) = \rho(\mathbf{\Omega}') I_\nu(\mathbf{\Omega}') + (1 - \rho(\mathbf{\Omega})) B_\nu(T_b). \tag{1.6}$$

If $\boldsymbol{n}$ denotes the outward normal vector, then $\mathbf{\Omega}' = \mathbf{\Omega} - 2(\boldsymbol{n} \cdot \mathbf{\Omega})\boldsymbol{n}$ denotes the reflected direction. The reflectivity ρ can be computed using Snell's and Fourier's law.

Finally, we use suitable initial values for T and I_ν.

1.1. Moment models

Before we present our key ideas we briefly review the basics of the moment approach. Consider again the transport equation (1.2) for the radiation. This equation is in fact a system of infinitely many coupled integro-differential equations that describes the distribution I_ν of all photons in time, space and velocity space. On the one hand this system is computationally very expensive and on the other hand we are not interested in the photon distribution itself but in macroscopic quantities like the mean energy or mean flux of the radiation field. For instance, only the integral of I_ν enters into the energy equation (1.1). The macroscopic quantities are moments of the distribution function. Let

$$\langle \cdot \rangle := \int_{\mathscr{S}} \int_0^\infty \cdot \, \mathrm{d}\nu \, \mathrm{d}\mathbf{\Omega} \tag{1.7}$$

denote the integral over all directions and frequencies. The directions are elements of the unit sphere $\mathscr{S}$ in three dimensions. The energy, flux vector and pressure tensor of the radiation field are defined, respectively, as

$$E := \langle I_\nu \rangle, \quad \boldsymbol{F} := \langle \mathbf{\Omega} I_\nu \rangle, \quad P := \langle (\mathbf{\Omega} \otimes \mathbf{\Omega}) I_\nu \rangle. \tag{1.8}$$

To derive equations for the macroscopic quantities we multiply the transport equation by 1 and $\mathbf{\Omega}$ and integrate over all directions and frequencies. We obtain the conservation laws:

$$\frac{1}{c}\partial_t E + \nabla \cdot \boldsymbol{F} = \kappa(aT^4 - E), \tag{1.9}$$

$$\frac{1}{c}\partial_t \boldsymbol{F} + \nabla \cdot P = -(\kappa + \sigma)\boldsymbol{F}. \tag{1.10}$$

We used Stefan–Boltzmann's law to replace $\langle B_\nu(T)\rangle$ by aT^4. These are four equations (the first is a scalar equation, the second has three components) for 10 unknowns (E scalar, $\boldsymbol{F}$ 3-component vector, P symmetric 3×3-matrix). Hence we have to pose an additional condition. Usually this condition is a constitutive equation for the highest moment P, expressed in terms of the lower moments E and $\boldsymbol{F}$. This is also referred to as closure. The simplest approximation, the so-called P_1 approximation, is obtained if we assume that the underlying distribution is linearly anisotropic. Thus we obtain $P = \frac{1}{3}E\,\mathrm{Id}$, where Id is the 3×3 unit tensor, and therefore:

$$\frac{1}{c}\partial_t E + \nabla \cdot \boldsymbol{F} = \kappa(aT^4 - E), \tag{1.11}$$

$$\frac{1}{c}\partial_t \boldsymbol{F} + \nabla \frac{1}{3}E = -(\kappa + \sigma)\boldsymbol{F}. \tag{1.12}$$

However, this approximation suffers from serious drawbacks. First, anisotropic situations are not correctly described. This becomes apparent most drastically for a ray of light with direction $\boldsymbol{\Omega}_0$, where $P = E\boldsymbol{\Omega}_0 \otimes \boldsymbol{\Omega}_0$. This problem remains for the P_N equations where it is assumed that the underlying distribution is a polynomial in $\boldsymbol{\Omega}$. Second, boundary conditions cannot be incorporated exactly. At a boundary we usually prescribe the ingoing flux only. Here we have to prescribe values for the full moments. These moments contain the unknown outgoing radiation. Various approximate boundary conditions have been introduced, cf. [22–24]. Moreover, a polynomial expansion cannot capture discontinuities in the angular photon distribution. Krook [16] remarks that especially at the boundary there is a discontinuity in the distribution between in- and outgoing particles.

In the following section we want to describe two key ideas which resolve these difficulties and have additional physically and mathematically desirable properties. The first idea is the entropy minimization principle that will be employed to obtain the constitutive equation for P. This principle has become the main concept of rational extended thermodynamics [27]. The second idea is to perform the integration not over all directions but only over parts of the unit sphere. Using this technique in combination with a kinetic scheme, more accurate boundary conditions can be formulated and discontinuities in the distribution can be taken care of.

1.2. Minimum entropy closure

We want to explain the entropy minimization principle and its practical application by means of our simple moment system (1.9) and (1.10). To close the system we determine a distribution function $\mathscr{I}_\nu$ that minimizes the radiative entropy

$$H_{\mathrm{R}}^*(I_\nu) = \int_{\mathscr{S}} \int_0^\infty h_{\mathrm{R}}^*(I_\nu)\,\mathrm{d}\nu\,\mathrm{d}\boldsymbol{\Omega} \tag{1.13}$$

with

$$h_{\mathrm{R}}^*(I_\nu) = \frac{2k\nu^2}{c^3}(n\log n - (n+1)\log(n+1)) \quad \text{where } n = \frac{c^2}{2h\nu^3}I_\nu \tag{1.14}$$

under the constraint that it reproduces the lower order moments,

$$\langle \mathscr{I}_\nu \rangle = E \quad \text{and} \quad \langle \boldsymbol{\Omega}\mathscr{I}_\nu \rangle = \boldsymbol{F}. \tag{1.15}$$

Some remarks on this principle might be in order. With a minus sign in front the entropy is maximized. It is then the well-known entropy for bosons adapted to radiation fields [28,32]. Furthermore, at first sight, it is not clear why the distribution should minimize the entropy when all that is known for non-equilibrium processes is that there exists an entropy inequality. But it can be shown [6] that the minimization of the entropy for given moments and the entropy inequality are equivalent. The above minimization problem can be solved explicitly and the pressure can be written as [7]

$$P = \left(\frac{1-\chi(\boldsymbol{f})}{2} \mathrm{Id} + \frac{3\chi(\boldsymbol{f})-1}{2} \frac{\boldsymbol{f} \otimes \boldsymbol{f}}{|\boldsymbol{f}|^2} \right) E. \tag{1.16}$$

Here, $\boldsymbol{f} = \frac{\boldsymbol{F}}{E}$ is the relative flux and

$$\chi(\boldsymbol{f}) = \frac{5 - 2\sqrt{4 - 3|\boldsymbol{f}|^2}}{3} \tag{1.17}$$

is the Eddington factor. In the literature, this Eddington factor has been derived based on many, apparently not connected, ideas. Levermore [21] assumed that there existed a reference frame in which the distribution was exactly isotropic and used the covariance of the radiation stress tensor. Anile et al. [1] derived it by collecting physical constraints on the Eddington factor and supposing the existence of an additional conservation law, where the conserved quantity behaves like the physical entropy near radiative equilibrium. Further variable Eddington factors have been proposed, cf. [26,21] and references therein.

Moreover, there are further desirable properties of this system. The flux is limited in a natural way, i.e., $|\boldsymbol{f}| \leqslant 1$. Physically, this corresponds to the fact that information cannot travel faster than the speed of light. Furthermore, the underlying distribution function is always positive. These two properties are not always preserved in many common approximations, e.g. diffusion approximations.

The moment system, closed by the entropy minimization principle, has a very important mathematical property. The system can be transformed to a symmetric hyperbolic system [1]. For symmetric hyperbolic systems one can prove the local well-posedness (i.e., existence, uniqueness and continuous dependence) of the Cauchy problem for smooth initial data [10].

In spite of its advantages the minimum entropy system still suffers from a major drawback. In Fig. 1 we show a numerical test case [4,9] with two colliding beams. We consider the domain $[0,1]$ with $\kappa = 2.5$, $\sigma = 0$. The temperature inside the medium is fixed at zero. At both sides, beams with a radiative temperature $T_R := (\frac{E}{a})^{1/4}$, where a is Stefan–Boltzmann's constant, of 1000 enter, i.e.,

$$I_\nu(0)|_{\mu>0} = aT_R^4 \frac{\delta(\mu-1)}{2\pi} \quad \text{and} \quad I_\nu(1)|_{\mu<0} = aT_R^4 \frac{\delta(\mu+1)}{2\pi}.$$

For this problem, the exact solution can be computed. The radiative energy is given by

$$E(x) = aT_R^4 \left(\mathrm{e}^{-\kappa x} + \mathrm{e}^{-\kappa(1-x)} \right).$$

Fig. 1 shows the radiative energy computed with the minimum entropy model (labeled "full moment") and the new model we propose (labeled "half moment"). The full moment model has a qualitatively wrong solution

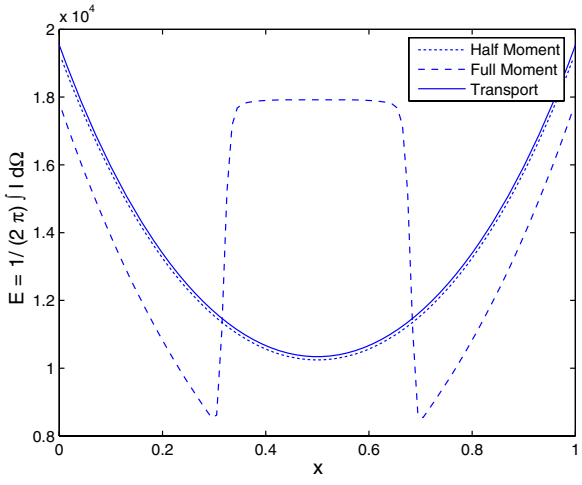

Fig. 1. Radiative energy in $[0,1]$ with $\sigma = 0$, $\kappa = 2.5$. Vanishing temperature, two beams entering at both sides. Artificial radiative shock wave in the full moment entropy (M_1) model.

with two shocks. This is not surprising since this Eddington factor, as stated above, is related to radiation which is isotropic in a certain frame [21]. This assumption is violated in the test case above. The unphysical behavior can be remedied by combining minimum entropy with the partial moment idea described in the following.

1.3. Partial moments

The partial moment idea is somehow intermediate between the discrete ordinates approach and moment models. In discrete ordinates models the integral over all directions is discretized with a numerical quadrature rule. This yields a coupled system of finitely many transport equations, each describing transport into one direction.

When we investigated the failure of the minimum entropy system in the last example, we saw that opposite beams cannot be handled correctly. An even simpler and more drastic example is the following. Consider a medium without absorption and without scattering bounded by two (infinite) parallel plates with different temperatures T_1 and T_2. Let $\boldsymbol{x}$ be the axis perpendicular to the plates. Then the solution to the transport equation is given by

$$I_\nu(\boldsymbol{\Omega}) = \begin{cases} B_\nu(T_1) & \text{if } \boldsymbol{\Omega}_x > 0, \\ B_\nu(T_2) & \text{if } \boldsymbol{\Omega}_x < 0, \end{cases} \tag{1.18}$$

where $\boldsymbol{\Omega}_x$ denotes the $\boldsymbol{x}$-component of the direction $\boldsymbol{\Omega}$. Obviously, if $T_1 \neq T_2$, the solution is discontinuous in $\boldsymbol{\Omega}$. This behavior cannot in principle be captured by any full moment method. This leads us to the following idea.

Let $\mathscr{A}$ be a partition of the unit sphere, where $A \in \mathscr{A}$ denotes the set of the angular integration. Instead of integrating over all directions we integrate over each $A \in \mathscr{A}$ separately. To that end we define the integral

$$\langle \cdot \rangle_A := \int_A \int_0^\infty \cdot \, \mathrm{d}\nu \, \mathrm{d}\boldsymbol{\Omega}. \tag{1.19}$$

Again, we multiply the transport equation by 1 and $\boldsymbol{\Omega}$ and integrate over each $A \in \mathscr{A}$ to obtain:

$$\frac{1}{c}\partial_t E_A + \nabla \cdot \boldsymbol{F}_A = \langle S \rangle_A, \tag{1.20}$$

$$\frac{1}{c}\partial_t \boldsymbol{F}_A + \nabla \cdot P_A = \langle \boldsymbol{\Omega} S \rangle_A. \tag{1.21}$$

The heat equation (1.1) can be written as

$$\rho_m c_m \partial_t T - \nabla \cdot (k \nabla T) = \kappa \left(\sum_{A \in \mathscr{A}} E_A - B(T) \right). \tag{1.22}$$

We define the corresponding partial moments by:

$$E_A = \langle I \rangle_A, \tag{1.23}$$

$$\boldsymbol{F}_A = \langle \boldsymbol{\Omega} I \rangle_A, \tag{1.24}$$

$$P_A = \langle (\boldsymbol{\Omega} \otimes \boldsymbol{\Omega}) I \rangle_A. \tag{1.25}$$

To close this system we have to find an equation for the partial pressures P_A as functions of the partial energies E_A and partial fluxes $\boldsymbol{F}_A$.

Examples for the choice of $\mathscr{A}$, which are used later, are:

- For the full moment model we have $A = \mathscr{S}$, i.e., the integral is over the full sphere.
- For the half moment model we have $A \in \{\mathscr{S}_+, \mathscr{S}_-\}$. Here, $\mathscr{S}_+ = \{\boldsymbol{\Omega} \in \mathscr{S} : \boldsymbol{\Omega}_x > 0\}$ is the positive half sphere, where the $\boldsymbol{x}$-component of $\boldsymbol{\Omega}$ is positive, and $\mathscr{S}_- = \{\boldsymbol{\Omega} \in \mathscr{S} : \boldsymbol{\Omega}_x < 0\}$ analogously is the negative half sphere.

- For the quarter moment model we have $A \in \{\mathscr{S}_{++}, \mathscr{S}_{+-}, \mathscr{S}_{--}, \mathscr{S}_{-+}\}$. Here, $\mathscr{S}_{++} = \{\mathbf{\Omega} \in \mathscr{S} : \mathbf{\Omega}_x > 0, \mathbf{\Omega}_y > 0\}$ is the quarter sphere in the first quadrant. Analogously, $\mathscr{S}_{+-} = \{\mathbf{\Omega} \in \mathscr{S} : \mathbf{\Omega}_x > 0, \mathbf{\Omega}_y < 0\}$, etc.
- In 3D, one could consider eight moments, for example $\mathscr{S}_{+++} = \{\mathbf{\Omega} \in \mathscr{S} : \mathbf{\Omega}_x > 0, \mathbf{\Omega}_y > 0, \mathbf{\Omega}_z > 0\}$, etc.

The separation between left- and rightgoing photons in 1D is clearly motivated. In more than one space dimension, the choice is not obvious, but we can name two guidelines. First, if the separations between the quadrants are aligned to the space grid, then a kinetic scheme for the solution to the equations becomes particularly simple. For a rectangular grid, the best choice in this sense the quarter moment model. This will be explained in Section 3.1. Second, the quarter moment model cannot produce unphysical shocks as the full moment model. This will be discussed in Section 3.2. In addition, the partition should be chosen depending on the physical problem at hand. The partial moment method allows the photon distribution to be discontinuous between the partitions. Hence the number and direction of the partitions should be chosen according to the expected form of the distribution. This will also be discussed in greater detail in Section 3.2.

The partial moment idea has appeared in the literature before, often under different names (like double-P_N) and mostly in connection with boundary conditions, for example recently in [4]. However, they were always combined only with the P_N closure. Schuster [34] and Schwarzschild [35] introduce two constant distributions for left- and rightgoing photons (P_0 approximation). Krook [16], based on ideas of Sykes [40], considers half moment in one space dimension with a P_N closure. Sherman [36] compares full-P_N and half-P_N numerically in 1D. Özisik et al. [29] derive a half moment P_1 closure in spherical geometry. Further references can be found in [25], where also an octuple P_1 closure in cylindrical geometry is introduced. Similar ideas appear in related subjects, like gas dynamics, cf. [5] and references therein.

Combining the partial moment idea with the minimum entropy closure, we will obtain a model that combines the advantages of both ideas and removes individual drawbacks.

2. Partial moment entropy approximation

For the sake of completeness we recall the explicit formulas mentioned earlier. We have to find a distribution function $\mathscr{I}_\nu$ that minimizes the radiative entropy

$$H_{\mathrm{R}}^*(I_\nu) = \int_{\mathscr{S}} \int_0^\infty h_{\mathrm{R}}^*(I_\nu)\,\mathrm{d}\nu\,\mathrm{d}\mathbf{\Omega} \tag{2.1}$$

with

$$h_{\mathrm{R}}^*(I_\nu) = \frac{2k\nu^2}{c^3}(n\log n - (n+1)\log(n+1)) \quad \text{where } n = \frac{c^2}{2h\nu^3} I_\nu \tag{2.2}$$

under the constraint that it reproduces the lower order partial moments,

$$\langle \mathscr{I}_\nu \rangle_A = E_A \quad \text{and} \quad \langle \mathbf{\Omega} \mathscr{I}_\nu \rangle_A = \boldsymbol{F}_A \tag{2.3}$$

for all $A \in \mathscr{A}$. The Lagrangian for this constrained minimization problem is

$$\mathscr{L}(I_\nu, \alpha, \boldsymbol{\beta}) = H_{\mathrm{R}}^*(I_\nu) - \sum_{A\in\mathscr{A}} \alpha_A(\langle I_\nu \rangle_A - E_A) - \sum_{A\in\mathscr{A}} \boldsymbol{\beta}_A \cdot (\langle \mathbf{\Omega} I_\nu \rangle_A - \boldsymbol{F}_A). \tag{2.4}$$

The coefficients $\alpha_A \in \mathbb{R}$ and $\boldsymbol{\beta}_A \in \mathbb{R}^3$ are the Lagrange multipliers corresponding to the constraints. The critical point $\mathscr{I}_\nu$ has to satisfy for all ΔI_ν

$$0 = \partial_{I_\nu} H_{\mathrm{R}}^*(\mathscr{I}_\nu)[\Delta I_\nu] - \sum_{A\in\mathscr{A}} \alpha_A \langle \Delta I_\nu \rangle_A - \sum_{A\in\mathscr{A}} \boldsymbol{\beta}_A \cdot \langle \mathbf{\Omega} \Delta I_\nu \rangle_A, \tag{2.5}$$

$$= \sum_{A\in\mathscr{A}} \int_A \int_0^\infty (\partial_{I_\nu} H_{\mathrm{R}}^*(\mathscr{I}_\nu) - \alpha_A - \boldsymbol{\beta}_A \cdot \mathbf{\Omega}) \Delta I_\nu \,\mathrm{d}\nu\,\mathrm{d}\mathbf{\Omega}. \tag{2.6}$$

Hence we obtain

$$\partial_{I_\nu} H_{\mathrm{R}}^*(\mathscr{I}_\nu) - \alpha_A - \boldsymbol{\beta}_A \cdot \mathbf{\Omega} = 0 \tag{2.7}$$

for each $A \in \mathscr{A}$. Solving for $\mathscr{J}_\nu$ we obtain after an appropriate rescaling of the multipliers the explicit formula

$$\mathscr{J}_\nu = \sum_{A\in\mathscr{A}} \mathscr{J}_{\nu,A} := \sum_{A\in\mathscr{A}} \frac{1}{\exp\left(\frac{h\nu}{k}\alpha_A(1+\boldsymbol{\beta}_A\cdot\boldsymbol{\Omega})\right)}\mathbf{1}_A, \tag{2.8}$$

where $\mathbf{1}_A$ is the characteristic function of the fraction A of the unit sphere. Averaging over all frequencies, we obtain according to the Stefan–Boltzmann law

$$\mathscr{J} = \sum_{A\in\mathscr{A}} \frac{1}{\alpha_A^4(1+\boldsymbol{\beta}_A\cdot\boldsymbol{\Omega})^4}\mathbf{1}_A. \tag{2.9}$$

Here we rescaled α_A again.

In the case of $\mathscr{A} = \{\mathscr{S}_+, \mathscr{S}_-\}$, the half moments over this distribution can be computed explicitly and moreover the half pressures can be expressed explicitly as functions of the half energies and half fluxes [9],

$$P_\pm = \frac{8f_\pm^2}{1\pm 6f_\pm + \sqrt{1\pm 12f_\pm - 12f_\pm^2}}E_\pm \mathrm{Id}. \tag{2.10}$$

For the full moment and the half moment model this explicit closure is possible only if we take the two lowest order moments. If we were to test with $\boldsymbol{\Omega}\otimes\boldsymbol{\Omega}$ and to obtain an equation for the pressure P an explicit closure would be impossible. A linearization of the minimum entropy distribution [38] ends up with a P_N closure and loses all the advantages of entropy minimization.

An additional difficulty arises if we consider quarter moments that are particularly suited for two space dimensions. Then even the integrals over the distribution function cannot be computed explicitly. However, the system can be closed numerically by tabulating the pressure tensor as a function of energy and flux. A fast and simple numerical procedure to obtain these tables is developed in the following section.

2.1. Quarter moments: numerical closure

In this section, we show how to obtain the quarter moment closure in two dimensions. This means that the distribution depends only on two space coordinates x, y and in angle it is symmetric with respect to the x–y plane. We will divide the sphere into the four quadrants, denoted by $++$, $+-$, $--$ and $-+$. The quarter moments will be denoted by

$$E_{ij}, \quad \boldsymbol{F}_{ij}, \quad P_{ij}, \tag{2.11}$$

where $i,j \in \{+,-\}$.

2.1.1. Preliminaries

Consider the entropy minimizer in the ij quarter space, where $i,j \in \{+,-\}$,

$$\mathscr{J}_{ij} = \frac{1}{a_{ij}^4(1+\boldsymbol{b}_{ij}\cdot\boldsymbol{\Omega})^4}. \tag{2.12}$$

The partial space moments are:

$$E_{ij} = \int_{ij} \frac{1}{a_{ij}^4(1+\boldsymbol{b}_{ij}\cdot\boldsymbol{\Omega})^4}\,\mathrm{d}\boldsymbol{\Omega}, \tag{2.13}$$

$$\boldsymbol{F}_{ij} = \int_{ij} \boldsymbol{\Omega}\frac{1}{a_{ij}^4(1+\boldsymbol{b}_{ij}\cdot\boldsymbol{\Omega})^4}\,\mathrm{d}\boldsymbol{\Omega}, \tag{2.14}$$

$$P_{ij} = \int_{ij} (\boldsymbol{\Omega}\otimes\boldsymbol{\Omega})\frac{1}{a_{ij}^4(1+\boldsymbol{b}_{ij}\cdot\boldsymbol{\Omega})^4}\,\mathrm{d}\boldsymbol{\Omega}. \tag{2.15}$$

The entropy minimizer is defined for all $\boldsymbol{b}_{ij}$ that satisfy $1+\boldsymbol{b}_{ij}\cdot\boldsymbol{\Omega} > 0$ for all $\boldsymbol{\Omega}$. It is easy to show that there is a bijection between the set of Lagrange multipliers,

$$\{(a_{ij}, \boldsymbol{b}_{ij}) : \ a_{ij} > 0 \text{ and } 1 + \boldsymbol{b}_{ij} \cdot \boldsymbol{\Omega} > 0 \text{ for all } \boldsymbol{\Omega}\} \tag{2.16}$$

and the set of physically realizable moments,

$$\{(E_{ij}, \boldsymbol{F}_{ij}) : \ E_{ij} > 0 \quad \text{and} \quad |\boldsymbol{F}_{ij}| < E_{ij}\}. \tag{2.17}$$

That every multiplier gives rise to a physically realizable moment can be directly seen from the formulas above. On the converse, that every physically realizable moment can be represented by the entropy minimizer is a consequence of the minimization procedure.

For the numerical inversion it is important that the mapping $(a_{ij}, \boldsymbol{b}_{ij}) \mapsto (E_{ij}, \boldsymbol{F}_{ij})$ can be reduced by one dimension. The relative flux,

$$\boldsymbol{f}_{ij} = \frac{\boldsymbol{F}_{ij}}{E_{ij}} = \frac{\int_{ij} \boldsymbol{\Omega} \frac{1}{(1+\boldsymbol{b}_{ij}\cdot\boldsymbol{\Omega})^4} \, \mathrm{d}\boldsymbol{\Omega}}{\int_{ij} \frac{1}{(1+\boldsymbol{b}_{ij}\cdot\boldsymbol{\Omega})^4} \, \mathrm{d}\boldsymbol{\Omega}}, \tag{2.18}$$

and the Eddington tensor,

$$D_{ij} = \frac{P_{ij}}{E_{ij}} = \frac{\int_{ij} (\boldsymbol{\Omega} \otimes \boldsymbol{\Omega}) \frac{1}{(1+\boldsymbol{b}_{ij}\cdot\boldsymbol{\Omega})^4} \, \mathrm{d}\boldsymbol{\Omega}}{\int_{ij} \frac{1}{(1+\boldsymbol{b}_{ij}\cdot\boldsymbol{\Omega})^4} \, \mathrm{d}\boldsymbol{\Omega}}, \tag{2.19}$$

depend only on $\boldsymbol{b}_{ij}$.

Our aim is now to construct a table of the Eddington tensor D_{ij} as a function of the relative flux $\boldsymbol{f}_{ij}$. To that end, we prescribe an admissible $\boldsymbol{F}_{ij}$, compute the Lagrange multiplier $\boldsymbol{b}_{ij}$ and hence obtain a value for D_{ij}.

2.1.2. Numerical inversion

In this section we explain how to obtain numerically a table for the Eddington tensor. For the sake of readability, we will drop the *ij* subscripts and only consider the ++ quarter space. In fact, we will only construct a table for this quadrant. The Eddington tensors for the other quadrants are obtained by symmetry considerations, which will be described at the end of the section.

We use spherical coordinates,

$$\boldsymbol{\Omega} = \begin{bmatrix} \sqrt{1-\mu^2}\cos\phi \\ \sqrt{1-\mu^2}\sin\phi \\ \mu \end{bmatrix}. \tag{2.20}$$

For the ++ quarter, μ runs in $[-1, 1]$ and ϕ runs in $[0, \pi/2]$. It is convenient to prescribe $\boldsymbol{f}$ and $\boldsymbol{b}$ in polar coordinates,

$$\boldsymbol{f} = \begin{bmatrix} |\boldsymbol{f}|\cos\varphi \\ |\boldsymbol{f}|\sin\varphi \\ 0 \end{bmatrix} \quad \text{and} \quad b = \begin{bmatrix} |\boldsymbol{b}|\cos\beta \\ |\boldsymbol{b}|\sin\beta \\ 0 \end{bmatrix}. \tag{2.21}$$

The third component of the flux (and also its Lagrange multiplier) is zero since we assumed a two-dimensional geometry. In the following, we will drop the third component, i.e., $\boldsymbol{F}$ as well as $\boldsymbol{f}$ will be 2-vectors and P will be a 2×2 matrix. The admissible values for the relative flux are then $0 < |\boldsymbol{f}| < 1$ and $0 < \varphi < \pi/2$. The integrals read

$$\boldsymbol{f} = \frac{\int_0^{\pi/2} \int_0^1 \begin{bmatrix} \sqrt{1-\mu^2}\cos\phi \\ \sqrt{1-\mu^2}\sin\phi \end{bmatrix} \frac{1}{(1+|\boldsymbol{b}|\sqrt{1-\mu^2}\cos(\beta-\phi))^4} \, \mathrm{d}\mu \, \mathrm{d}\phi}{\int_0^{\pi/2} \int_0^1 \frac{1}{(1+|\boldsymbol{b}|\sqrt{1-\mu^2}\cos(\beta-\phi))^4} \, \mathrm{d}\mu \, \mathrm{d}\phi} \tag{2.22}$$

and

$$D = \frac{\int_0^{\pi/2} \int_0^1 \begin{bmatrix} (1-\mu^2)\cos^2\phi & (1-\mu^2)\sin\phi\cos\phi \\ (1-\mu^2)\sin\phi\cos\phi & (1-\mu^2)\sin^2\phi \end{bmatrix} \frac{1}{(1+|\boldsymbol{b}|\sqrt{1-\mu^2}\cos(\beta-\phi))^4} \, \mathrm{d}\mu \, \mathrm{d}\phi}{\int_0^{\pi/2} \int_0^1 \frac{1}{(1+|\boldsymbol{b}|\sqrt{1-\mu^2}\cos(\beta-\phi))^4} \, \mathrm{d}\mu \, \mathrm{d}\phi}. \tag{2.23}$$

To obtain good starting values for the inversion we create a table of $\boldsymbol{f}$ as a function of $|\boldsymbol{b}|$and β. Given $|\boldsymbol{b}|$ and β we check if these values are admissible, i.e., whether $1 + \boldsymbol{b} \cdot \boldsymbol{\Omega} > 0$ for all $\boldsymbol{\Omega}$. Note that this can be done analytically. After that we compute the above integrals numerically. For example, this can be done in a comfortable way by using standard integration routines like `quad` from `matlab`.

To create the final tables, we choose a grid for $|\boldsymbol{f}|$, φ. At first we exclude the boundaries $|\boldsymbol{f}| = 0, 1$ and $\varphi = 0, \frac{\pi}{2}$, since the integrals are not defined for these values. Then we obtain a starting approximation for $|\boldsymbol{b}|$, β by inverse interpolation in the above table. With this value we start a nonlinear system solving routine, for example `matlab`'s `fzero` to obtain $|\boldsymbol{b}|$, β. With these values we compute D. For $|\boldsymbol{f}| = 0, 1$ the Eddington tensor D can be computed explicitly. The distribution function is respectively isotropic or a Dirac. Values for $\varphi = 0, \frac{\pi}{2}$ can be approximated well by extrapolation. The result of this procedure is shown in Fig. 2, where we show D_{yy} as a function of $|\boldsymbol{f}|$ and φ.

Now we explain how the other quadrants can be handled by symmetry considerations. Let $D_{++}(\boldsymbol{f}_{++})$ denote the $++$ Eddington tensor depending on $\boldsymbol{f}_{++}$. For example, we obtain the $+-$ Eddington tensor in the following way. Let R denote the matrix representation of the rotation by $\frac{\pi}{2}$ (counter-clockwise). Then

$$D_{+-}(\boldsymbol{f}_{+-}) = R^{\mathrm{T}} D_{++}(R\boldsymbol{f}_{+-})R. \tag{2.24}$$

The other quadrants are handled analogously. Only R has to be replaced by the matrix rotating the relative flux into the $++$ quadrant.

The natural question arises how fine we have to discretize $|\boldsymbol{f}|$ and φ. We want to obtain a table that is accurate enough for all physical situations not destroying the advantages of the minimum entropy approach. On the other hand, the table should be as small as possible since it has to be evaluated in every step of the numerical computations. For the numerical examples presented in Section 3 we investigated the dependence on the size of the tables. In our experience, a discretization of $(|\boldsymbol{f}|,\varphi)$ on a 30×30 grid is sufficient.

2.2. Properties of the partial moment entropy system

The partial moment entropy approximation, especially the quarter moment case which we concentrated on, has a lot of desirable physical and mathematical properties that we want to sum up here:

- The underlying distribution function is always positive. Hence the relative flux and the speed of propagation are limited, in agreement with special relativity.
- The system is symmetriziable hyperbolic. This makes it accessible to a powerful mathematical theory guaranteeing well-posedness locally in time.
- Like the full moment entropy approximation [7], the system approaches the diffusive limit and correctly represents one beam, in the sense that the Eddington factor is zero for $|\boldsymbol{f}| = 0$ and $D_{yy} = 1$ for $|\boldsymbol{f}| = 1$ and $\varphi = \pi/2$, i.e., flux into the y-direction.

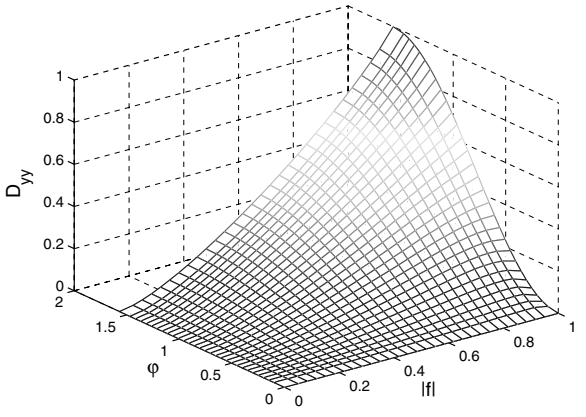

Fig. 2. Component D_{yy} of the Eddington tensor as a function of $(|\boldsymbol{f}|,\varphi)$.

- The eigenvalues of the half moment and quarter moment entropy approximation have a special structure. For the half moment case, the eigenvalues of the "+" direction are always positive, the eigenvalues of the "−" direction are always negative. This agrees well with our physical intuition of right- and leftgoing photons. The same is true for the quarter moment system in the following sense. Let us write the equations for one quarter in the general form

$$\partial_t U + \partial_x F(U) + \partial_y G(U) = S(U). \tag{2.25}$$

  For the "++" quarter, the Jacobian matrices $F'(U)$ and $G'(U)$ have only positive eigenvalues. For the "+−" quarter, $F'(U)$ has only positive eigenvalues while $G'(U)$ has only negative eigenvalues, analogously for the other quarters.
- The minimum entropy method leads to problems in the field of rarefied gas dynamics if moments of higher order are used [13,14]. This fact is related to the unbounded velocity space. Hence it is not an issue here if we take only angular moments. If one wants to treat also frequency-dependent coefficients, one could use moments of the distribution in terms of frequency, cf. [37]. But then the existence of a minimum entropy solution cannot be guaranteed.
- This property makes very simple and accurate numerical schemes possible, for example kinetic schemes or upwind schemes. Also, an implicit discretization has a very simple structure.

When we compare our model to other existing models the question arises whether the two lowest order moments E and $\boldsymbol{F}$ are sufficient. One reason for choosing only the lower moments is that we wanted to obtain an accurate and yet in terms of computational cost competitive model. In two space dimensions with quarter moments this leads to 12 variables. Direct discretizations of the transport equation usually use many directions [15] leading sometimes to over 100 variables. Taking more moments would make the model too expensive. A criterion for the number of moments has been put forward by Struchtrup [38]. He determines the number of moments by taking an incoming beam and supposing that this beam is correctly represented if the eigenvalues of the moment system are close to the speed of light. For the P_N closure he obtains $N \approx 30$ as a sufficient condition. Due to the special form of the distribution function, in our nonlinear approximation the propagation speed automatically approaches the speed of light for a beam. Thus, according to this criterion, the two lower order moments are sufficient.

3. Numerical results

In times of ever increasing code complexity, code verification becomes much more important. Recently, the Method of Manufactured Solutions [33] has been suggested as a tool for code verification. The direct application of the Method of Manufactured Solutions is very difficult to use in our case, since due to the numerical closure, the model itself is only known numerically. However, we have performed the following dynamic tests, as put forward in [33]:

- *Trend tests:* We know how the solution changes if we vary absorption and scattering coefficients, initial temperature and boundary temperature. In addition, we observed convergence of the spatial grid.
- *Symmetry tests:* The solution should be symmetric for symmetric data. In our case, we also rotated initial and boundary data by 90 degrees steps. This tests symmetries between the four quarter spaces.
- *Method of exact solutions:* In several special cases, one can compute an exact solution to the quarter moment entropy model. One example is the two beam case in Fig. 1. The Eddington tensor is known analytically for a beam ($|\boldsymbol{f}| = 1$) and for equilibrium. In this way, exact solutions can be constructed.
- *Comparison tests:* In Section 3.2, we show comparisons with other established codes.

We consider several steady test cases. We compare the radiative energy E obtained with the following methods:

- *Transport:* Solution with a discrete ordinates (S_N) approximation, cf. [15]. We consider this to be the true solution.

- *Quarter space:* Solution obtained with the quarter moment entropy model.
- *SP3:* The SP_3 approximation is a higher order diffusion approximation, cf. [20] for details.
- *P1:* The well-known P_1 approximation.

The Rosseland approximation gives in all cases considered far less accurate results.

3.1. Numerical methods

The *Transport* solution has been obtained with a multilevel iteration method [2,3]. The angular discretization is a C-60 discretization (with 60 directions), cf. [15]. The parabolic SP1 equations have been discretized with a standard finite difference scheme. The first order partial differential equations, P1 and the *quarter moment model*, that come out from the moment method need a special treatment, especially at the boundary. In the following we want to present a kinetic scheme for the partial moment model in two dimensions.

We want to adopt the viewpoint of finite volume schemes. Consider a cell $\mathscr{Z}_i$ and denote the set of all neighboring cells by $\mathscr{N}_i$. Let n_{ij} be the outward normal from cell $\mathscr{Z}_i$ to cell $\mathscr{Z}_j$ and let K_{ij} be the edge between cell i and j. Furthermore, denote by $|\mathscr{Z}_i|$ the area of the cell $\mathscr{Z}_i$, cf. Fig. 3. The partial moments are constant functions on each cell. Assume that we discretize some partial flux term, e.g. $\nabla \cdot \boldsymbol{F}_A$. Averaging over the cell and using Gauss' theorem yields

$$\frac{1}{|Z_i|}\int_{\mathscr{Z}_i} \nabla \cdot \boldsymbol{F}_A \,\mathrm{d}x = \frac{1}{|Z_i|}\int_{\partial\mathscr{Z}_i} \boldsymbol{n}\cdot\boldsymbol{F}_A \,\mathrm{d}s = \frac{1}{|Z_i|}\sum_{j\in\mathscr{N}_i}\int_{K_{ij}} \boldsymbol{n}_{ij}\cdot\boldsymbol{F}_A \,\mathrm{d}s. \tag{3.1}$$

The integral over the edge can be approximated by the midpoint rule,

$$\frac{1}{|Z_i|}\sum_{j\in\mathscr{N}_i}\int_{K_{ij}} \boldsymbol{n}_{ij}\cdot\boldsymbol{F}_A \,\mathrm{d}s \approx \frac{1}{|Z_i|}\sum_{j\in\mathscr{N}_i} |K_{ij}|\boldsymbol{n}_{ij}\cdot\boldsymbol{F}_{A,ij}, \tag{3.2}$$

where $\boldsymbol{F}_{A,ij}$ is some value of $\boldsymbol{F}_A$ on the edge K_{ij}.

The key idea of the kinetic scheme is to approximate this normal flux in the following way. In each cell $\mathscr{Z}_i$ we have, by means of the closure, a distribution function $\mathscr{J}_i$. The partial flux over the cell boundary is assumed to consist of the outgoing partial flux from the cell $\mathscr{Z}_i$ and the incoming partial flux from the cell $\mathscr{Z}_j$. Thus we get

$$\boldsymbol{F}_{A,ij} \approx \int_{A\cap\{\boldsymbol{n}_{ij}\cdot\boldsymbol{\Omega}<0\}} \boldsymbol{\Omega}\mathscr{J}_j \,\mathrm{d}\boldsymbol{\Omega} + \int_{A\cap\{\boldsymbol{n}_{ij}\cdot\boldsymbol{\Omega}>0\}} \boldsymbol{\Omega}\mathscr{J}_i \,\mathrm{d}\boldsymbol{\Omega}. \tag{3.3}$$

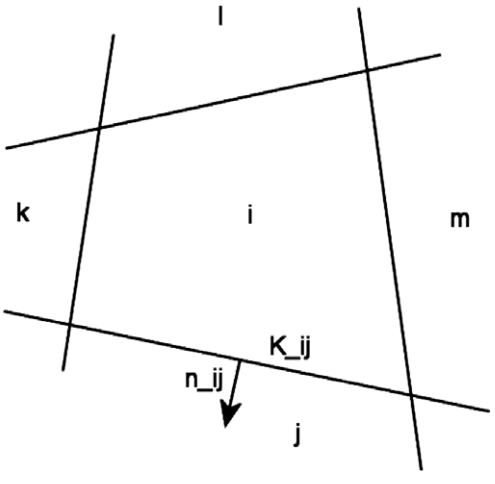

Fig. 3. Finite volume scheme.

These integrals in general do not coincide with the partial moments themselves. A further approximation is

$$\boldsymbol{F}_{A,ij} \approx \frac{|A \cap \{\boldsymbol{n}_{ij} \cdot \boldsymbol{\Omega} < 0\}|}{|A|} \boldsymbol{F}_{A,j} + \frac{|A \cap \{\boldsymbol{n}_{ij} \cdot \boldsymbol{\Omega} > 0\}|}{|A|} \boldsymbol{F}_{A,i}. \tag{3.4}$$

The factors in front of the partial fluxes are the relative overlap of the incoming/outgoing flux directions and the partial space A. For a rectangular grid parallel to the axes, the relative overlap is either 0 or 1 and thus Eq. (3.4) holds exactly. Thus a kinetic scheme for the quarter moment model becomes very simple, since the fluxes over the cell boundaries are just sums of the unknowns. Boundary conditions can be implemented by placing ghost cells at the boundary, which contain the prescribed distribution.

After discretizing in space we obtain a system of ordinary differential equations which can be solved by standard methods. All of the latter systems have eigenvalues in modulus less than the speed of light. Thus, similar CFL conditions hold. To be valid in the diffusive limit, the kinetic schemes can be modified to become asymptotic preserving. For a more detailed review on kinetic schemes we refer the reader to [12,39] and references therein. The scheme presented above is of first order. For the construction of higher order schemes, see [13,30].

3.2. Steady test cases

In this section we present some numerical examples probing different regimes.

In the first two test cases we consider the unit square $D = [0,1]^2$ and a fixed temperature profile, $T(x,y) = 1000 + 400(x+y)$. We do not consider the material equation (1.1), but instead prescribe a fixed temperature profile. In the following we always consider the steady solution. As the ingoing radiation at the boundary we prescribe a Planckian at the corresponding temperature T. The results for the intermediate regime, $\sigma = 1$ and $\kappa = 1$, are shown in Fig. 4. The quarter moment entropy method outperforms the diffusive approximations. The differences become more striking in the transport regime, $\sigma = 0.1$ and $\kappa = 0.01$, shown in Fig. 5. The temperature profile is anisotropic. This cannot be captured by diffusion approximations that smear out anisotropies. Our model is capable of capturing the anisotropies and agrees with the transport solution.

In our third example, we consider the rectangular domain $D = [0,1] \times [0,10]$ divided into the subdomains $D_0 = [0.45, 0.55] \times [4.5, 5.5]$ and $D \backslash D_0$. Temperature and scattering coefficient are discontinuous, $T = 1000$ and $\kappa = 1$ in D_0, $T = 1800$ and $\kappa = 0.1$ outside D_0. The result is shown in Fig. 6. Again, the quarter moment model is the best approximation.

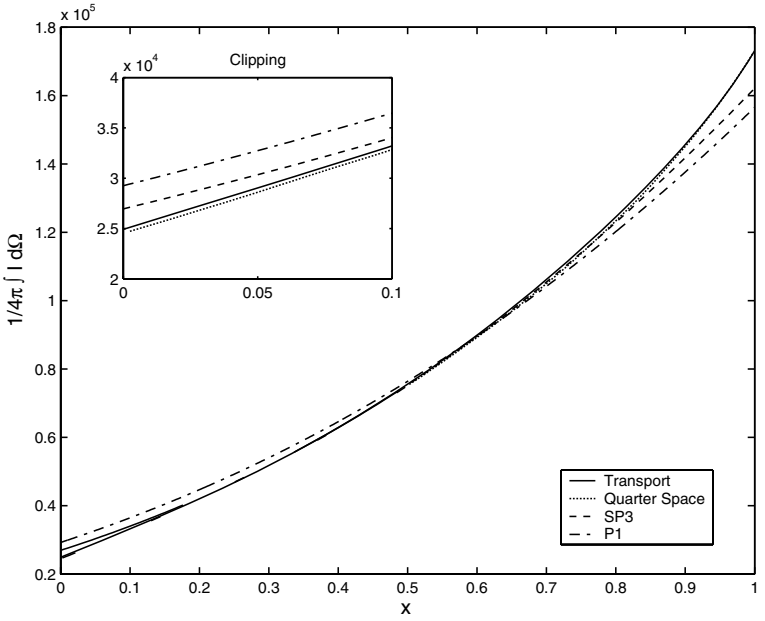

Fig. 4. Steady radiative energy for a fixed matter temperature profile in $[0,1]^2$, $T(x,y) = 1000 + 400(x+y)$, Planckian at boundary. Intermediate regime, $\sigma = 1$, $\kappa = 1$. Plot along the diagonal $x = y$.

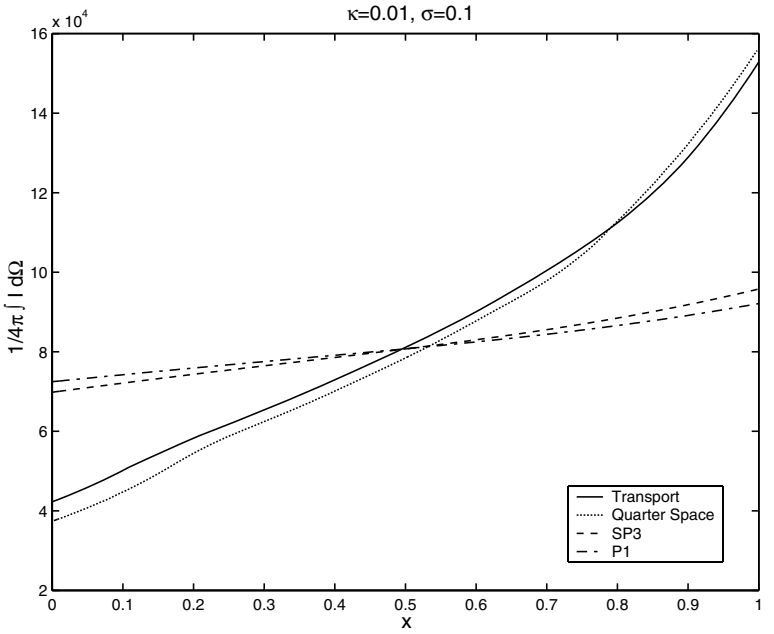

Fig. 5. Steady radiative energy for a fixed matter temperature profile in $[0,1]^2$, $T(x,y) = 1000 + 400(x+y)$, Planckian at boundary. Transport regime, $\sigma = 0.1$, $\kappa = 0.01$. Plot along the diagonal $x = y$.

In our fourth example, we do not fix the temperature and consider both the material equation and the radiative transfer equation. We set $\rho_m c_m = 1$, $k = 1$ and $h_B = 1$. The boundary temperature is set to $T_b(x,y) = 1000 + 800x$. This defines the boundary value for the material temperature as well as the ingoing blackbody radiation. The results are shown in Fig. 7. Although the heat conduction adds diffusion, the quarter moment entropy model again outperforms the diffusion approximations.

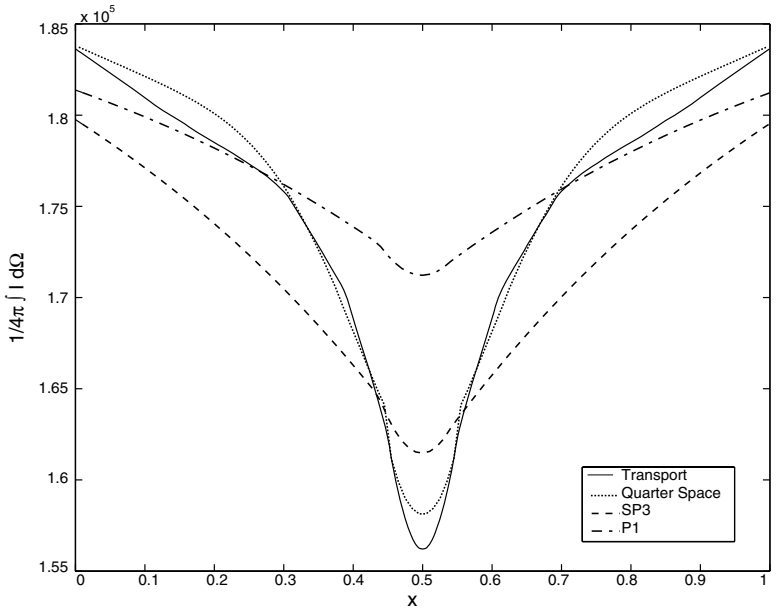

Fig. 6. Steady radiative energy for a fixed matter temperature profile and discontinuous coefficients, $T(x,y) = 1000$ and $\kappa = 1$ in D_0, $T(x,y) = 1800$ and $\kappa = 0.1$ outside D_0. Planckian at boundary. Scattering coefficient $\sigma = 1$. Plot along $y = 5$.

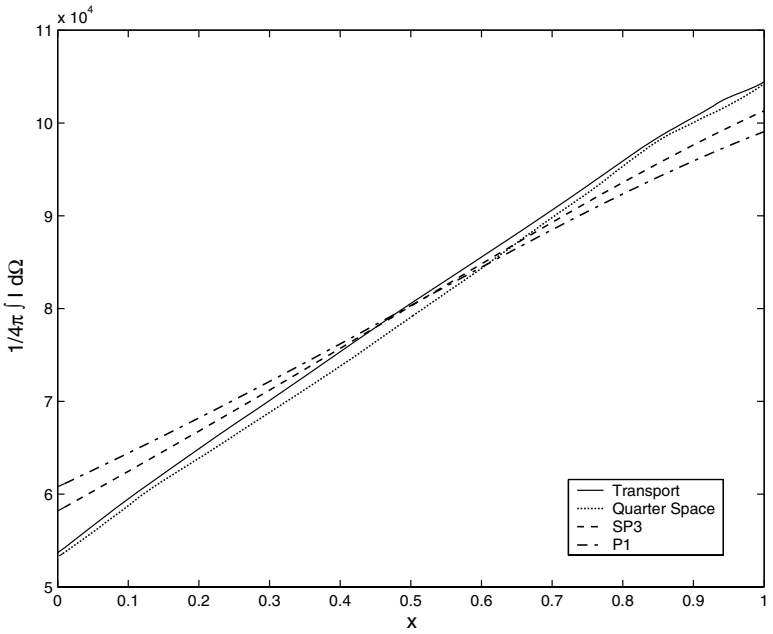

Fig. 7. Steady radiative energy for the coupled equations in $[0,1]^2$. Boundary temperature $T_b(x,y) = 1000 + 800x$, Planckian at boundary. Intermediate regime, $\sigma = 1$, $\kappa = 1$.

In our fifth example, we investigate how our model represents beams. We consider the unit square $[0,1]^2$. The temperature is zero, absorption is small, $\kappa = 0.01$, no scattering, $\sigma = 0$. At the left boundary and at the lower boundary, two beams with spatial width 0.1 enter the domain. We prescribe the beams in the $++$ direction,

$$E_{++} = aT^4_{\text{Beam}} \quad \text{and} \quad \boldsymbol{F}_{++} = \begin{bmatrix} \cos\phi \\ \sin\phi \end{bmatrix} E_{++} \tag{3.5}$$

with $\phi = 0$ and $\phi = \frac{\pi}{2}$, respectively. The result is shown in Fig. 8. We have plotted the lines of constant radiative energy. First the beams penetrate the medium and are correctly described by our model. When they meet roughly in the middle of the square, both partial fluxes in the $++$ quadrant add up to one flux pointing into the diagonal direction. The two beams cannot be exactly described by the underlying distribution function. The effect is that the beams do not penetrate each other as they should, but the energy smears out.

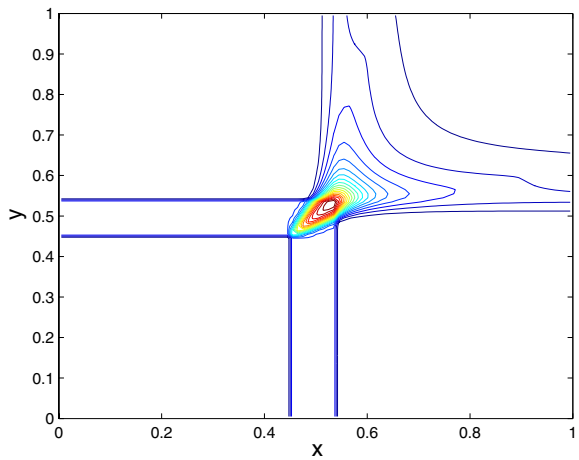

Fig. 8. Contour plot of the radiative energy. Transport regime, $\sigma = 0.01$ and $\kappa = 0.01$. Temperature $T = 0$. Beams entering from the left and from the bottom.

Several conclusions can be drawn from this example. First, we note that this is a very extreme test case. Most approximate models, especially diffusion and full moment models, perform worse. If the beam direction is not exactly aligned with one of the discrete directions, even high order discrete ordinates solutions, although maintaining the beam structure better, have some diffusion.

In contrast to the two beam case shown in Fig. 1, in which the full moment minimum entropy model produced an unphysical shock, the quarter moment minimum entropy model produces no artificial shock. The solution is just smeared out, i.e., the solution does not become qualitatively completely wrong. This is due to the fact that in the quarter moment model no two opposing fluxes can add up to zero. There exists no reference frame in which the distribution has to be isotropic.

The test was designed such that both beams were in the same quadrant. If one rotates the coordinate system (or the quarters) then both beams are in different quadrants. When they meet, they correctly penetrate through each other without interacting, because in the absence of scattering the equations for the quarter moments decouple. The quarter moment model allows the angular distribution to be discontinuous. If for a certain physical problem one knows in advance, in which directions the distribution has maxima or changes rapidly, one can rotate the angular domain in a suitable way. Of course this means on the one hand that a code with a fixed angular decomposition (e.g. quarter moments) is limited in its applicability. On the other hand, one can construct examples of beam configurations in which the quarter moments cannot be rotated such that there is exactly one beam in each quadrant.

The fact that the solution changes if we rotate the coordinate system (and/or the quadrants of integration) means that the solution to the quarter moment model is not rotationally invariant. In the discrete ordinates method this property gives rise to the ray effect. Information is just propagated along the predefined directions. Moment models on the other hand, are rotationally invariant. If the data is rotated then the solution just rotates. Our model is in some sense intermediate between moment models and discrete ordinates.

This can be seen by the test in Fig. 9. We consider the domain $[0,1]^2$ with temperature $T = 0$, no influx at the boundary. Inside is a small circle of radius 0.05 with temperature $T = 1000$. Absorption and scattering are small, $\sigma = \kappa = 0.1$. We compare the solution obtained with the quarter moment minimum entropy model to the result obtained with a discrete ordinates solution with 8 directions (thus the same number of equations). In the discrete ordinates solution, the energy from the hot source is just transported into the 8 fixed directions. This explains the bumps in Fig. 9, where we show the radiative energy along $y = 0.2$. The bumps are at the points where two of the characteristic directions intersect with the line $y = 0.2$. The quarter moment minimum entropy model does not have these qualitatively wrong bumps. However, the solution has some smaller fluctuations. In two dimensions, our model is a hyperbolic system of order 8. However, the characteristic curves

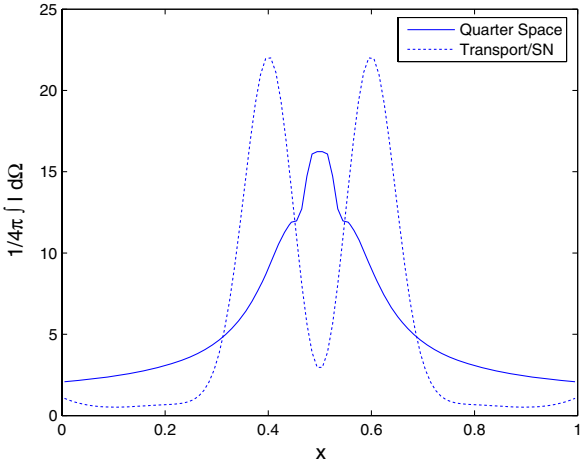

Fig. 9. Ray effect in quarter moment minimum entropy model and S8 solution. Domain $[0,1]^2$ with temperature $T = 0$, a circle of radius 0.05 with temperature $T = 1000$, no influx. Transport regime, $\sigma = \kappa = 0.1$. Shown is the radiative energy along $y = 0.2$.

depend on the solution and need not be straight lines. This shows that the quarter moment minimum entropy model has a ray effect but it is rather small.

4. Conclusions

- The combination of the minimum entropy closure and the partial moment idea created a simple and accurate model that can compete also in terms of computational cost with existing models. The model is in some sense intermediate between discrete ordinates models which split up the directions and moment models which integrate over all directions. On the one hand it can describe anisotropies better than full moment models or diffusion, but on the other hand it has a limited ray effect. Thus, when applying our model, one should have in mind the types of anisotropies which are present in the problem. A large number of beams should be treated rather by a ray-tracing method.
- The nonlinear minimum entropy closure guarantees a higher accuracy than the usual linear P_N closure. The unphysical shock in the minimum entropy system is removed.
- Numerical experiments and a simple criterion suggest that the two lowest order moments are sufficient to describe most physical regimes.
- The model naturally has many physically and mathematically advantageous properties, e.g. flux limitation, the correct limiting behavior in diffusive as well as free-streaming regimes, symmetric hyperbolicity and a simple and natural eigenvalue structure.
- The quarter moment model, as it was presented in this paper, is particularly suited for rectangular geometries. The kinetic scheme is particularly simple. Boundary conditions can be prescribed in a natural way. However, the general formulation of the partial moment approach includes general geometries. If the angular partition is chosen to fit the physical problem at hand, the approximation becomes better.

5. Future work

- The gray half moment model has been generalized to frequency-dependent coefficients by using a multigroup approach [43], see also [42] for a detailed investigation of multigroup models. It is straightforward to generalize the partial moment entropy model to this case. Just consider the partial integrals over a part of the sphere and a frequency interval,

$$\langle\cdot\rangle_{A,i} := \int_A \int_{\nu_{i-\frac{1}{2}}}^{\nu_{i+\frac{1}{2}}} \cdot \, \mathrm{d}\nu \, \mathrm{d}\mathbf{\Omega}. \tag{5.1}$$

  The entropy minimizer is then a sum over all $A \in \mathscr{A}$ and over all bands i,

$$\mathscr{J}_\nu = \sum_i \sum_{A\in\mathscr{A}} \frac{1}{\exp(\frac{h\nu}{k}\alpha_{A,i}(1+\boldsymbol{\beta}_{A,i}\cdot\mathbf{\Omega}))} 1_A 1_i. \tag{5.2}$$

- The generalization to three dimensions using octuple moments is also straightforward. Also the idea of using only half moments in multi-D should be investigated. Half moments are sufficient to remove the unphysical shock from the minimum entropy system and the number of equations is smaller. An "adaptive" half moment model is considered in [31].
- Semi-transparent boundary conditions, which are important, e.g. in glass manufacturing, can easily be incorporated. All we need to do is integrate Eq. (1.6) over each $A \in \mathscr{A}$. The integrals have to be tabularized again.
- Recent results [17,11] indicate that it is critical for a model or numerical scheme to preserve the linear and quadratic infinite medium solutions to the transport equation. It was conjectured that this is a necessary condition for a scheme to perform well in the diffusive limit. The question, whether the kinetic scheme for the quarter moment minimum entropy model satisfies this property, has to be investigated.
- Further applications of the model are currently under investigation. The coupling to hydrodynamics will be of special interest.

Acknowledgments

The authors thank the two anonymous referees for their helpful comments. This work was supported by the German Research Foundation DFG under Grant KL 1105/14/2 and the IHP project HPRN-CT-2002-00282 of the European Union.

References

[1] A.M. Anile, S. Pennisi, M. Sammartino, A thermodynamical approach to Eddington factors, J. Math. Phys. 32 (1991) 544–550.
[2] C.T. Banoczi, C.T. Kelley, A fast multilevel algorithm for the solution of nonlinear systems of conductive–radiative heat transfer equations, SIAM J. Sci. Comput. 19 (1998) 266–279.
[3] C.T. Banoczi, C.T. Kelley, A fast multilevel algorithm for the solution of nonlinear systems of conductive–radiative heat transfer equations in two space dimensions, SIAM J. Sci. Comput. 20 (1999) 1214–1228.
[4] T.A. Brunner, J.P. Holloway, One-dimensional Riemann solvers and the maximum entropy closure, J. Quant. Spectrosc. Radiat. Transf. 69 (2001) 543–566.
[5] P.-J. Clause, M. Mareschal, Heat transfer in a gas between parallel plates: moment method and molecular dynamics, Phys. Rev. A 38 (1988) 4241–4252.
[6] W. Dreyer, Maximisation of the entropy in non-equilibrium, J. Phys. A 20 (1987) 6505–6517.
[7] B. Dubroca, J.L. Feugeas, Entropic moment closure hierarchy for the radiative transfer equation, CR Acad. Sci. Paris Ser. I 329 (1999) 915–920.
[8] B. Dubroca, M. Frank, A. Klar, G. Thömmes, Half space moment approximation to the radiative heat transfer equations, ZAMM 83 (2003) 853–858.
[9] B. Dubroca, A. Klar, Half moment closure for radiative transfer equations, J. Comput. Phys. 180 (2002) 584–596.
[10] A.E. Fischer, J.E. Marsden, The Einstein evolution equations as a first-order quasi-linear hyperbolic system I, Commun. Math. Phys. 26 (1972) 1–38.
[11] H.L. Hanshaw, The Multidimensional Multiple Balance Method for SN Radiation Transport, Ph.D. Thesis, University of Michigan, Ann Arbor, 2005.
[12] M. Junk, Kinetic Schemes: A New Approach and Applications, Ph.D. Thesis, Universität Kaiserslautern, 1997.
[13] M. Junk, Maximum entropy for reduced moment problems, Math. Meth. Mod. Appl. Sci. 10 (2000) 1001–1025.
[14] M. Junk, A. Unterreiter, Maximum entropy moment systems and galilean invariance, Continuum Mech. Thermodyn. 14 (2002) 563–576.
[15] R. Koch, W. Krebs, S. Wittig, R. Viskanta, The discrete ordinate quadrature schemes for multidimensional radiative transfer, J. Quant. Spectrosc. Radiat. Transf. 53 (1995) 353–372.
[16] M. Krook, On the solution of equations of transfer, Astrophys. J. 122 (1955) 488.
[17] E.W. Larsen, Infinite-medium solutions of the transport equation, SN discretization schemes, and the diffusion equation, Tranp. Theory Stat. Phys. 32 (2003) 623–643.
[18] E.W. Larsen, J.B. Keller, Asymptotic solution of neutron transport problems for small mean free path, J. Math. Phys. 15 (1974) 75.
[19] E.W. Larsen, G. Thömmes, A. Klar, New frequency-averaged approximations to the equations of radiative heat transfer, SIAM J. Appl. Math. 64 (2003) 565–582.
[20] E.W. Larsen, G. Thömmes, A. Klar, M. Seaïd, T. Götz, Simplified P_n approximations to the equations of radiative heat transfer in glass, J. Comput. Phys. 183 (2002) 652–675.
[21] C.D. Levermore, Relating Eddington factors to flux limiters, J. Quant. Spectrosc. Radiat. Transf. 31 (1984) 149–160.
[22] J.C. Mark, The Spherical Harmonics Method, Part I, Tech. Report MT 92, National Research Council of Canada, 1944.
[23] J.C. Mark, The Spherical Harmonics Method, Part II, Tech. Report MT 97, National Research Council of Canada, 1945.
[24] R.E. Marshak, Note on the spherical harmonic method as applied to the milne problem for a sphere, Phys. Rev. 71 (1947) 443–446.
[25] M.P. Mengüc, R.K. Iyer, Modeling of radiative transfer using multiple spherical harmonics approximations, J. Quant. Spectrosc. Radiat. Transf. 39 (1988) 445–461.
[26] G.N. Minerbo, Maximum entropy Eddington factors, J. Quant. Spectrosc. Radiat. Transf. 20 (1978) 541–545.
[27] I. Müller, T. Ruggeri, Rational Extended Thermodynamics, second ed., Springer-Verlag, New York, 1993.
[28] A. Ore, Entropy of radiation, Phys. Rev. 98 (1955) 887.
[29] M.N. Özisik, J. Menning, W. Hälg, Half-range moment method for solution of the transport equation in a spherical symmetric geometry, J. Quant. Spectrosc. Radiat. Transf. 15 (1975) 1101–1106.
[30] B. Perthame, Kinetic Formulation of Conservation Laws, Oxford University Press, Oxford, 2002.
[31] J.-F. Ripoll, A.A. Wray, A half-moment model for radiative transfer in a 3d gray medium and its reduction to a moment model for hot, opaque sources, J. Quant. Spectrosc. Radiat. Transf. 93 (2005) 473–519.
[32] P. Rosen, Entropy of radiation, Phys. Rev. 96 (1954) 555.
[33] K. Salari, P. Knupp, Code Verification by the Method of Manufactured Solutions, Tech. Report SAND2000-1444, Sandia National Laboratories, 2000.
[34] A. Schuster, Radiation through a foggy atmosphere, Astrophys. J. 21 (1905) 1–22.
[35] K. Schwarzschild, Über das Gleichgewicht von Sonnenatmosphären, Akad. Wiss. Göttingen, Math. Phys. Kl. Nachr. 195 (1906) 41–53.

[36] M.P. Sherman, Moment methods in radiative transfer problems, J. Quant. Spectrosc. Radiat. Transf. 7 (1967) 89–109.
[37] H. Struchtrup, An extended moment method in radiative transfer: the matrices of mean absorption and scattering coefficients, Ann. Phys. (NY) 257 (1997) 111–135.
[38] H. Struchtrup, On the number of moments in radiative transfer problems, Ann. Phys. (NY) 266 (1998) 1–26.
[39] H. Struchtrup, Kinetic schemes and boundary conditions for moment equations, Z. Angew. Math. Phys. 51 (2000) 346–365.
[40] J.B. Sykes, Approximate integration of the equation of transfer, Month. Notices Roy. Astron. Soc. 111 (1951) 377.
[41] R. Turpault, Construction d'une modèle M1-multigroupe pour les équations du transfert radiatif, CR Acad. Sci. Paris Ser. I 334 (2002) 1–6.
[42] R. Turpault, A consistent multigroup model for radiative transfer and its underlying mean opacities, J. Quant. Spectrosc. Radiat. Transf. 94 (2005) 357–371.
[43] R. Turpault, M. Frank, B. Dubroca, A. Klar, Multigroup half space moment approximations to the radiative heat transfer equations, J. Comput. Phys. 198 (2004) 363–371.